8-10-2020

Characteristics of Flow and Heat Transfer in Horizontal Channel with Mounted Rectangular Cross Section Bars.

M. Mohamed
Mechanical Power Engineering Department, Faculty of Engineering, Mansoura University, Mansoura, Egypt, msafwat@mans.edu.eg

Elsayed Elshafei
Mechanical Power Engineering Department, Faculty of Engineering, Mansoura University, Mansoura, Egypt, eelshafei@mans.edu.eg

Hamada Yousef
M. Sc. Student Mechanical Power Engineering Department, Faculty of Engineering, Mansoura University, Mansoura, Egypt, hamada_wes@yahoo.com

Follow this and additional works at: https://mej.researchcommons.org/home

Characteristics of Flow and Heat Transfer in Horizontal Channel with mounted Rectangular Cross section Bars

خواص السريان وانتقال الحرارة فى قناة افقية مع وجود قضبان مستطيلة المقطع

M. Safwat Mohamed [a], Elsayed A. M. Elshafei [a] and Hamada A. Yousef [b]

Mechanical Power Engineering Department, Faculty of Engineering,
Mansoura University, El-Mansoura 35516, Egypt

[a] E-mail: eelshafei@mans.edu.eg, msafwat@mans.edu.eg
[b] M.Sc. Student, E-mail: hamada_wes@yahoo.com

ملخص البحث:

فى هذا البحث تم دراسة خصائص السريان و انتقال الحرارة من أربعة قضبان مستطيلة ذات مقاطع مختلفة مسخنة بواسطة فيض حرارى ثابت وأنتقال الحرارة كان بالحمل الجبرى والسريان كان مضطربا وغير انضغاطى لمدى رقم رينولدز من ١٥٠٠٠ الى ٣٥٠٠٠ و نسبة الانسداد (d/H) ١٦٧،٠ ، ١٣٣،٠ ، ١،٠ ، ٠٦٧،٠ ، ونسبة الطول الى العرض (c/d) ١ ، ١،٢٥ ، ١،٦٧ ، ٢،٥ و القدرة الداخلة (input Power) ٤١،٤ ، ٥٣،١٦ ، ٦٦،٤ w وكانت الدراسة معملية وعددية بأستخدام كود ديناميكا الموائع الحسابية (Fluent) وأستخدام نموذج الاضطراب $\left(Rng\ K - \varepsilon \right)$. تم دراسة تأثير تغير معدل الحرارة المضافة ورقم رينولدز على رقم نسلت وشكل توزيع السرعات خلف القضبان حيث أثبتت النتائج المعملية أن انتقال الحرارة المتمثل فى رقم نسلت يتأثر بقوة بكلا من رقم رينولدز(Re) و نسبة الانسداد (d/H) ونسبة الارتفاع الى العرض (c/d) ولا يتأثر بقوة بالقدرة الداخلة (input Power) وتم المقارنة مع باحثين أخرين وكان هناك اتفاق جيد. أثبتت النتائج المعملية ايضا أن توزيع السرعة خلف القضبان يتأثر بكل من رقم رينولدز (Re) ونسبة الانسداد(d/H) ونسبة الطول الى العرض (c/d) . أثبتت المقارنة بين النتائج المعملية و النتائج العددية فى الدراسة الحالية وجود اتفاق جيد بينهما.

Abstract

Experimental and Numerical investigations in fluid flow and heat transfer have been carried out to study the effect of blockage ratio (d/H) and aspect ratio (c/d) due to flow separation around rectangular bars. The turbulent flow and forced convection heat transfer characteristics for an incompressible and steady flow past rectangular bars were carried out. The Reynolds numbers was varied from 1.5×10^{4} up to 3.5×10^{4}, blockage ratios of 0.167, 0.133, 0.1 and 0.067, aspect ratios of 1, 1.25, 1.67 and 2.5 and input power of 41.4, 53.16 and 66.4W. The velocity profiles and forced convection heat transfer coefficient were predicted numerically using Fluent code. The two equations of turbulence model (RNG K-Epsilon) were employed in this investigation. The experimental results showed that Nusselt number is strongly affected by both blockage ratio and Reynolds number. Nusselt number was not strongly affected by the power (heat flux). The experimental results also showed that the velocity distribution behind the bars is affected by blockage ratio, aspect ratio and Reynolds number. The numerical and experimental results of the present work were compared with available literature data and showed good agreement.

Nomenclature

A_s	surface area, m^2		T_{out}	air outlet temperature, K
c	width of rectangular bar, m		T_m	air mean temperature, K
c/d	aspect ratio of the rectangular bar		T_{sur}	duct wall surface temperature, K
d	height of rectangular bar, m		T_{th}	thermocouple temperature, C$^\circ$
d/H	blockage ratio of the rectangular bar		T_u	turbulence intensity
D_H	hydraulic diameter, m		u	velocity in x-direction, m/s
G_{rw}	Grashof number		v	velocity in y-direction, m/s
h	heat transfer coefficient, W/m^2 K		V	heater electric voltage, Volts
H	height of the wind tunnel, m		x_o	distance in x-direction, m
I	heater electric current, A		y_o	distance in y-direction, m
K	thermal conductivity, W/m K			
l	bar length, m			Greek symbols
L	test section length, m		α	Thermal diffusivity, m^2/s
Nu	Nusselt number, hd/k		Δp	pressure difference, p$_a$
P	pressure, p$_a$		$\delta_{i,j}$	Kronecker delta
P_h	heater power input, W			
Pr	Prandtl number, v/α (=0.71)		ε_s	emissivity
Q	total heat transfer rate, W		κ	von Karman constant (= 0.4)
Q_r	heat transfer losses by radiation, W		μ	Viscosity, kg/m s
Re	Reynolds number, ud/v		v	kinematic viscosity of air, m^2/s
T_{in}	air inlet temperature, K		ρ	density, kg/m^3
T_s	bar surface temperature, K		σ	Stefan-Boltzmann constant, W/m^2 K^4

1. Introduction

The geometry of bluff bodies plays a pivotal role in the flow-structure interactions, the resulting flow and pressure fields and heat transfer around them. For rectangular bars, the separation and reattachment characteristics of the flow are controlled by the bar aspect ratio and the approach flow turbulence. This investigation is relevant to many practical engineering applications such as Heat exchangers, cooling of electronic components, automobiles, air conditioning spacecraft and aircraft.

H. Reiher [1] carried out experimental studies on fluid flow and heat transfer around square cylinder with different ratios of the angles of attack 0° and 45° and in range of Re between 1960: 6000. R. Hilpert [2] also carried out experimental studies on fluid flow and heat transfer around square cylinder with different ratios of the angles of attack 0° and 45° for a range of Re between 3900 : 78500. T. Igarashi [3] carried out experimental studies on fluid flow and heat transfer around square cylinder 15, 20 and 30 mm with different ratios of the angles of attack 0° and 45°, in range of Re between 5600 : 56000 and the turbulence level in the working section was less than 0.5%. Local heat transfer coefficient distribution around a square cylinder using thermocouples was measured. T. Igarashi [4] carried out experimental studies on fluid flow and heat transfer around square cylinder 30 mm with different ratios of the angles of attack from 0° to 45° for a range of Re between 5600 : 56000 and the turbulence level in the working section was less than 0.5%, and

local heat transfer coefficient distribution around a square cylinder using thermocouples. They observed that Nu is directly proportional to Re and inversely proportional to angle of attack. T. Igarashi [3] and T. Igarashi [4] found that the heat transfer coefficients were closely related to the drag coefficients.

T. Igarashi [5] investigated the fluid flow and heat transfer around rectangular cylinder. In this experiment the following parameters were taken: (1) Re=7500 ~ 37500, (2) aspect ratio (c/d) of the section ranging from 0.33~1.5 and the turbulence level in the working section was less than 0.5%. The author had established the correlation between Nusselt number and Reynolds number on the side and rear faces of the rectangular cylinder and these were $Nu_s = C_sRe^{2/3}$ and $Nu_b = C_bRe^{2/3}$. From the experiment, the author had noticed that the above constants C_s, C_b varies with the ratio c/d and had a maximum at the critical geometry, c/d= 0.67 and also noticed that the heat transfer coefficients on the rear face of cylinder was higher than other faces and average heat transfer coefficient was proportional to the r.m.s of fluctuating pressure.

Flow and heat transfer around three different rectangular bars were numerically simulated with the standard k-epsilon turbulence model by Valencia and Orellana [6]. The modified version of the k-epsilon model yields to lower local and global Nusselt number predictions than the standard version. The oscillation of the Nusselt number on the side faces decreased strongly with c/d. The prediction of local heat transfer rates was poor in separated regions compared with experimental results around the bar.

Valencia [7] performed a numerical study to compute the heat transfer and friction in a channel with a mounted square

bar of different sizes detached from the channel wall. The Reynolds number based on channel height ranged from 10000 to 100000, whereas the bar height to channel height (d/H) varied from 0.15 to 0.35. The enhancement of mean heat transfer ranged between 11% and 53% with d/H between 0.15 and 0.35 respectively.

Valencia [8] numerically investigated the heat transfer enhancement in a channel with a built-in square cylinder in laminar flow. It was observed that Nu increased by 46% for cylinder with d/H=0.5 and about 11% for the cylinder with d/H=0.25 at Re=1000.

Lyn el al. [9] using LDV (laser doppler velocimetry) technique, measured velocity components and turbulence quantities for turbulent flow of water around a square cylinder with blockage ratio of 7% at Re=2.2x10⁴. Phase (ensemble)-averaged velocity and turbulence intensities were presented in various locations along the top surface of the obstacle as well as within the wake region downstream of the obstacle.

Ahmed and Yovanovich [10] studied the external forced convection heat transfer from isothermal bodies of different shapes over a range of $10^4 \le Re \le 10^5$. In case of horizontal square cylinder, scatter in results between them and the others was reported. They argued that to the difference in T_u, G_{rw}, and the temperature difference between the surface and the ambient.

Sparrow et al. [11] reported the previous study for non-circular, circular cylinders and spheres in cross-flow. In case of square cylinder, it was reported that the best representation of the average Nusselt number versus Re is $Nu= 0.14\ Re^{0.66}$ for $5000 \le R_e \le 60000$, which was that recommended [3].

Goldstein et al [12] measured local mass transfer from a square cylinder and its base

plate using a naphthalene sublimation technique, the cross section of the test section was 610 mm wide and 305 mm high, and air speed varied from nominally 8.7 to 17.9 m/s corresponding to $1.36 \times 10^4 \leq Re \leq 2.8 \times 10^4$. The freestream turbulence intensity was less than 0.6% over the entire range of speeds. Mass transfer data were compared with heat transfer data of Igarashi [3]. It was concluded that the average values of heat and mass transfer are in good agreement with other.

Yoo et al. [13] investigated local and average mass transfer rates from a rectangular cylinder having various width to height ratios using naphthalene sublimation technique, The experimental apparatus comprised a wind tunnel, naphthalene casting facility and a sublimation depth measurement system. Mass transfer data were compared with those of heat transfer which were obtained using thermocouples in the constant heat flux boundary condition.

Dhiman et al [14] investigated the effect of Peclet number ($0.7 \leq Pe \leq 4000$) and blockage ratio (1/8, 1/6 and 1/4) on the flow and heat transfer characteristics of a square cylinder confined in a planar channel with Reynolds number ($1 \leq Re \leq 45$) in the 2D steady flow regime. They observed that the average Nusselt number increases monotonically with an increase in the Reynolds number and/or Prandtl number.

Moussaoui et al [15] investigated numerically the two-dimensional flow and heat transfer, in a horizontal channel differentially heated and obstructed by an inclined square cylinder mounted to the approaching flow with an angle of inclination equal to 45° for Reynolds number ranging from 0 to 300 at Prandtl number, Pr = 0.71. They observed that the local Nusselt number changes only in the rear end of the inclined square prism due to the vortex shedding created by the presence of the

obstacle. The average Nusselt number was found to be an increasing function of the Reynolds number. The influence of the Re was more significant in the presence of the inclined square cylinder. The maximum enhancement of heat transfer was about 58% for Re equal to 300 in the presence of the inclined square cylinder.

Rao et al [16] investigated the effect of power-law fluid behavior ($0.2 \leq n \leq 1$) on the flow and heat transfer phenomena for a square cylinder with 45° incidence where n is the *flow behavior index* (dimensionless). The two-dimensional steady flow regime, with ($0.1 \leq Re \leq 40$) and ($0.7 \leq Pr \leq 100$), with two boundary conditions, constant wall temperature and constant heat flux were considered. They observed that the Nusselt number for the constant heat flux condition was generally higher than that for the constant wall temperature condition under identical conditions.

Abd [17] studied experimentally free and forced heat transfer from three cylinders of different cross-sections circular, triangular and square in cross flow of air. The heat transfer coefficient was calculated for forced convection with several Reynolds number ranges of (4555-18222). The study covered free convection impact for values of Rayleigh number ranging between (1069-3321). It was found that in the case of forced convection, the heat transfer of the triangular cylinder was better than that of the square and circular cylinder. For the triangular cylinder, it was found, the best case of heat transfer was achieved when the triangle cylinder faces opposite to air flow. The square cylinder (tilted angle 45°) had a better heat transfer than that of the square cylinder when it lies on one of its width. In the case of free convection the best position of the triangular cylinder was found where the triangle cylinder faced down ward.

The purpose of the present study is to study the effect of blockage ratio (d/H), aspect ratio (c/d) and Reynolds number (Re) on the heat transfer and fluid flow characteristics around rectangular cross bars experimentally and numerically using CFD codes.

2. Experimental Set-up

The schematic layout of the experimental set-up is shown in Fig. 1. A low turbulence open-type wind tunnel having an axial fan is used in the experiments. The wind tunnel has a variable frequency controller for the motor and a remote speed control device to control the air speed in the test section. These reduce the free-stream turbulence to less than 0.5% at air velocity up to 62 m/s as mentioned in the manual. Air is drawn at room temperature, and passes through filters, honeycombs damping screens, and a 12.5 to 1.0 contraction section. Constant area straight duct of length 0.3 m is attached at the test section inlet.

2.1 Test Section

A photograph of the test section is shown in Fig.2. The dimensions of the test section are 0.3 m high, 0.3 m wide and 1 m long respectively. The air flow velocity through the test section varies from 4.8m/s to 19.7m/s. The bars are located at the channel axis and located at x_o=0.45 m from the inlet of test section and y_o =0.15 m as shown in Fig.3.

2.2 Rectangular Bars

The tested bars geometrical parameters are listed in Table 1. These bars have 250 mm long, spanned the wind tunnel and are made of steel 37. The whole surface of the bars was covered with a stainless steel sheet 0.02mm thick. They were heated under constant heat flux using heater fitted to the

bar. The surface temperatures of the bar were measured with 14 "T" Type copper-constantan thermocouples, 1mm diameter buried in the circumference wall 6mm depth as shown in Fig.4 and Fig. 5.

Table 1: Geometrical parameters of tested bars

H(cm)	d(cm)	c(cm)	d/H	c/d
30	2	5	0.067	2.5
30	3	5	0.1	1.67
30	4	5	0.133	1.25
30	5	5	0.167	1

2.3 Measurements

The used measuring instruments are described in the following sub-section.

2.3.1 Temperature measurements

The surface temperatures of the rectangular bars, inlet and outlet average air temperatures are measured using calibrated (T) type copper-constantan thermocouples as shown in Fig. 6 . The signal outputs of these thermocouples were obtained by data logger device (model PIC101-N OPERATING INSTRUCTIONS) which has an accuracy of ± 0.25 % and 0.1C° resolution. Fig.6 Shows the relation between thermocouple readings and thermometer readings and the equation obtained is T (C°) = 0.95 T_{th} (C°) - 0.54

2.3.2 Velocity measurements

A traversing mechanism, Pitot tube and digital micro-manometer are used to measure the air velocities behind the cross bars. The air velocity is given by

$$u = 1.29\sqrt{\Delta P} \qquad\qquad\qquad (1)$$

The Pitot tube can be moved in the vertical and horizontal direction in the test section by the traversing mechanism mounted on the upper wall of test section. The Pitot tube was connected to a digital micro-monometer

(model 530 ALNOR). This micro-manometer can read the positive and negative values of pressure difference with an accuracy of ± 0.25 % and 1.0 Pa resolution. The relative uncertainty of air velocity was found to be equals to 0.25%.

2.4 Experimental procedure

The experimental procedure is made as follows:

1- The bar is fixed in its place in the test section and the electric heater is connected to electric source passing via an electric voltage stabilizer to get constant heat flux. .

2- Connect the autotransformer (variac) and wattmeter in series, to calculate the energy required for the electrical heater. Thermocouples are connected with the temperature recorder passing through switch to read the temperature at each point separately.

3- Run the wind tunnel and adjust the frequency to give the air speed equivalent to the four Reynolds numbers required .

4- Adjust the voltage to give required heat input from heater and wait to get the steady state which takes from 70 to 90 minutes depending on the surface area of the bar, air velocity and the heat input from the heater .

5- Take the inlet and outlet air temperature readings and temperature readings at 14 points of the surface of the bar.

6- Take air velocity distribution for four fixed sections behind the bar x/c =2, 2.8, 3.6 and 4.4 respectively as follows

   a- Move the pitot-tube horizontally by the traversing mechanism at first section then move it vertically to get the velocity distribution at 30 points at this section.

   b- Repeat step (a) at other positions.

7- Repeat steps from 3 to 6 for other Reynolds numbers.

8- Repeat steps from 1 to 7 for other bars.

2.5 Temperature distribution

Temperature distribution over the bars surface was measured by 14 T type thermocouples distributed on the bar surfaces. Average air temperature is measured using two thermocouples, one is located at 20 cm upstream of the bar and the other at about 2 cm downstream of the bar. All thermocouples were calibrated and connected with a temperature recorder via a selector switch.

The rate of input heat to the bar can be calculated as:

$$P_h = IV \qquad \text{.....................} \quad (2)$$

The rate of heat loss due to radiation is given by:

$$Q_r = \sigma \varepsilon_s A_s \left[(T_s)^4 - (T_{sur})^4 \right] \qquad \text{............} \quad (3)$$

The net heat rate from the surface to air flowing over the bar can be written as:

$$Q = P_h - Q_r \qquad \text{............................} \quad (4)$$

The convective heat transfer coefficient can be calculated as:

$$h = \frac{Q}{A(T_s - T_m)} \qquad \text{......................} \quad (5)$$

Where the mean temperature, T_m is given by.

$$T_m = \frac{T_{in} + T_{out}}{2} \qquad \text{.........................} \quad (6)$$

Nusselt number can be calculated as:

$$Nu = \frac{hd}{k}$$ .... (7)

2.6 Velocity Distribution

Velocity distribution behind the bars can be obtained by using the standard pitot-tube which is used to measure the pressure difference. The air velocity is given by equation (1).

Reynolds number can be calculated as.

$$Re = \frac{uD_H}{v}$$ .... (8)

3. Numerical Model

The computational domain and the boundary conditions are sketched in Fig 7. At the inlet, the flow enters with a streamwise component $u=u_{in}$, $v=0$ and $T=T_{in}$. The Re based on the bar height are varied between 1.5×10^4 and 3.5×10^4, and a turbulence level less than 0.5%. The blockage ratios, d/H, are varied and taken as 0.067, 0.1, 0.13 and 0.167, respectively. The bar is located at the channel axis with $x_o/H = 1.5$ and $y_o/H = 0.5$. At the outlet the streamwise gradients of all variables are set to zero

3.1. Governing conservation equations

Fluid flow and Heat transfer characteristics around a rectangular bars mounted in the horizontal channel are governed by the Navier-Stokes equations. For turbulent flows, the flow field in the channel is assumed to be steady, two-dimensional nonisothermal, incompressible (Mach number < 0.4), and the fluid is assumed to be Newtonian with constant properties.

- **Continuity:**

$$\frac{\partial u_j}{\partial x_j} = 0.$$ .... (9)

- **Momentum:**

$$\frac{\partial}{\partial x_j}\left(\rho u_i u_j\right) = -\frac{\partial p}{\partial x_i}$$
$$+ \frac{\partial}{\partial x_j}\left((\mu + \mu_t)\left(\frac{\partial u_i}{\partial x_j} + \frac{\partial u_j}{\partial x_i}\right) - \frac{2}{3}\rho \kappa \delta_{i,j}\right)$$

.... (10)

- **Energy:**

$$\frac{\partial(\rho u_j T)}{\partial x_j} = \frac{\partial}{\partial x_j}\left((\Gamma + \Gamma_t)\frac{\partial T}{\partial x_j}\right)$$

.... (11)

Where the turbulent viscosity μ_t, diffusion coefficient Γ and the turbulent diffusion coefficient Γ_t are given by:

$$\mu_t = \rho C_\mu(\frac{k^2}{\varepsilon}), \quad \Gamma = \frac{\mu}{Pr}, \quad \Gamma_t = \frac{\mu_t}{Pr_t}$$

.... (12)

3.2. Turbulence Model

Several turbulence models can be used. In the present analysis, the RNG k-ε turbulence model is employed. The following one the RNG k-ε equation.

- **Turbulent kinetic energy:**

$$\rho U_i \frac{\partial k}{\partial x_i} = \mu_t S^2 + \frac{\partial}{\partial x_i}\left((\mu + \frac{\mu_t}{\sigma_k})\frac{\partial k}{\partial x_i}\right) - \rho\varepsilon$$

.... (13)

- **Dissipation rate:**

$$\rho U_i \frac{\partial \varepsilon}{\partial x_i} = C_{1\varepsilon}\left(\frac{\varepsilon}{k}\right)\mu_t S^2 + \frac{\partial}{\partial x_i}\left((\mu + \frac{\mu_t}{\sigma_\varepsilon})\frac{\partial \varepsilon}{\partial x_i}\right) - C_{2\varepsilon}\rho\left(\frac{\varepsilon^2}{k}\right)$$

.... (14)

Where

$$S \equiv \sqrt{2S_{ij}S_{ij}}, \quad S_{ij} \equiv \frac{1}{2}\left(\frac{\partial U_j}{\partial x_i} + \frac{\partial U_i}{\partial x_j}\right)$$

.... (15)

Where C_μ, $C_{1\varepsilon}$ and $C_{2\varepsilon}$ are the model constants, and σ_k and σ_ε are the turbulent Prandtl numbers for k and ε, respectively. These constants have the following default values:

$C_\mu = 0.0845, C_{1\varepsilon} = 1.42, C_{2\varepsilon} = 1.68$;

$\sigma_k = 0.7194$ and $\sigma_\varepsilon = 0.7194$

In the above equations steady, incompressible flow without body forces are assumed.

3.3. Grid independence test

The flow and temperature fields are computed numerically using CFD (Fluent 6.3.26). The computer program has been developed to solve the above equations to obtain Reynolds number, Temperature and the velocity distribution.

The preferred procedure for determining the most accurate mesh is to carry out test runs on different mesh sizes. Fig. 9 shows the mean values of Nusselt number of bar surface grid sizes 100x200, 110x235, and 120x295 compared with Ahmed [10] The results of grid size 100x200 has high difference with the results of Ahmed [10]. While grid sizes 110x235 and 120x295 give good agreement. So the grid size 110x235 is selected for low time consuming.

3.4. Validation of the model

To validate the present model, a comparison between present numerical approach and experimental study of Lyn et al. [9] using the Fluent (6.3.26) are shown in Fig.10. It can be seen that the velocity distribution behind the square bar is fairly close to that reported by Lyn et al. [9].

4. Results and discussion

The experimental and numerical results of characteristics flow and heat transfer in horizontal channel mounted with rectangular bars are discussed in the following subsections.

4.1 Experimental Results

4.1.1 Flow characteristics:

The flow characteristics around rectangular bars have been studied by measuring the velocity distribution behind the bars. As shown in Fig. 11, it is observed that the velocity distribution varies with the aspect ratio (c/d), blockage ratio (d/H) and Reynolds number (Re). For all aspect ratios the turbulence intensity increases near the bars, and decreases as long as the measurements are taken far from the bar. Fig. 11 also indicates that as the aspect ratios increase the wake behind the bar is getting narrower.

Figure (12) shows the effect of Re on the wake flow behind the bars. As shown in fig. (12) the wake flow is directly proportional to the Reynolds number.

4.1.2 Heat transfer characteristics

- Square Bar:

Figure 13 shows Nu versus Re at three different values of power rate 66.4W, 53.16W and 41.45W, respectively. This experiment was conducted on the square bar (c/d=1).The figure shows that the Nusselt number is not strongly affected by the variation of power input rate.

Figure 14 shows comparisons between the present experimental studies, with the available experimental data in the literature. Present results seem logical when compared with Ahmed [10]. The blockage ratio in the present study is 16.6% greater than that reported by Ahmed (5.6%). The present experimental values of Nu are about 5.4% less than those of Ahmed [10]. The turbulence intensity in the present study is less than 0.5% while in Ahmed [10] it was in the range of 2.2% up to 4.6%. Therefore the present results are acceptable when compared with Ahmed [10] as can be seen in Fig.14.

The present experimental values of Nu are about 12.3% less than those of Igarashi [3]. Although the turbulence intensity in the present experimental equal to Igarashi [3] (less than 0.5%). The present blockage ratio gives 16.6% greater than that readed by Igarashi [3] (about 7.5%, no effect to Blockage ratio in Igarashi [3]) this is unacceptable.

- Rectangular Bars:

Figure 15 shows the Nusselt number versus Re at different aspect ratios. It can be observed that Nusselt number is directly proportional to both the blockage ratio and Reynolds number, and inversely proportional to the aspect ratio.
The present experimental results can be correlated as:

$$Nu = 0.33 \mathrm{Re}^{0.6} \mathrm{Pr}^{0.3} [c/d]^{-0.25} [d/H]^{0.13}$$

$$\dots\dots\dots\dots\dots\dots\dots\dots\dots\dots\dots \text{(16)}$$

With a maximum error of $\pm 7.5\%$

4.2 Numerical Results

Turbulent kinetic energy and Dissipation rate equations are solved using CFD (fluent 6.3.26) for detecting flow characteristics.

4.2.1 Fluid flow characteristics

The effect of the aspect ratio (c /d), blockage ratio (d/H) and Reynolds number (Re) on one hand and effect of the turbulence areas behind the bars on the other hand, have the same trend of both the experimental results and numerical results. For all aspect ratios the turbulent intensity increases near the bars, and reduces if it is measured far from the bars as shown in Fig.16. It can be observed that as the aspect ratios increases the wake behind the bar is getting narrower.

The same trend of the experimental results as that of numerical results is obtained where the turbulence intensity behind the bars is directly proportional to the Reynolds number as shown in Fig. 17.

4.2.2 Heat transfer characteristics:

The effect of bar cross sectional on the rate of heat transfer exchanged between heated bar and air flow can be seen in Fig.18.

For Square cross sectional bar, it can be seen that the Nusselt number is directly proportional to Reynolds number.

For Rectangular cross sectional Bars, the trend of the numerical results is the same as that for the experimental results where the Nusselt number is directly proportional with both the blockage ratio, Reynolds number,

and inversely proportional with the aspect ratio.

At the same value of Reynolds number, the rate of heat transfer from square cross sectional bar is seen to be higher than the rate of heat transfer from rectangular cross sectional bar

4.3   Comparison   between experimental   and   numerical results:

4.3.1 Fluid flow characteristics

Figure 19 shows the velocity distribution for both   experimental   and   Numerical predictions. It can be seen that both results are very close.

4.3.2 Heat transfer characteristics

Figure 20 shows a comparison between experimental and numerical results for the rate of heat transfer exchanged between the tested   heated   cross   bars   of   different geometries (c/d ranging from 1 up to 2.5) and air flowing over them. It can be seen that there is a fair agreement between them.

5. Conclusions

Characteristics of flow and heat transfer in   a   horizontal   channel   fitted   with rectangular cross bars heated under constant heat flux are numerically and experimentally investigated. The cross bars with different geometries (blockage ratios of 0.167, 0.133, 0.1 and 0.067 and aspect ratios of 1, 1.25, 1.67 and 2.5, respectively over a range of Reynolds number ($1.5 \times 10^4 \leq Re \leq 3.5 \times 10^4$). From the obtained results, the following may be concluded:

i- Nusselt number is not strongly affected by the input power rate.

ii- Nusselt number is directly proportional to the blockage ratio(d/H), Reynolds number, and inversely proportional to the aspect ratio (c/d).

iii-The experimental data of heat transfer are correlated as:

$Nu = 0.33 \mathrm{Re}^{0.6} \mathrm{Pr}^{0.3} [c/d]^{-0.25} [d/H]^{0.13}$ with   a maximum error of $\pm 7.5\%$ in the tested range of   Reynolds   number   and   the investigated geometrical parameters of the bars. The relative uncertainty for Nu is 0.0143% and for Re is 0.25%.

iv- The wake flow behind the bars is affected by aspect ratio (c /d), blockage ratio (d/H) and Reynolds number. For all aspect ratios the turbulence intensity increases near the bars, and reduces if it is measured far from the bars. With increasing aspect ratios, the wake behind the bar is getting narrower. In the mean time the turbulent intensity of flow is directly proportional to the Reynolds number

v- The effect of cross bar geometry and Reynolds number on flow and heat transfer characteristics resulted from the numerical investigation is the same as that assured by the experimental one.

vi- The numerical predictions for both Nu and velocity distribution fairly agreed with those detected from the experimental results.

References

1- H. Reiher, "Der warmeubergang von stromender luft an rohrbundel in kreuzstrom", VDI Forschungsheft 269, 1926, 47.

2- R.   Hilpert,   "Warmeabgabe   von heheizten drahten und rohrem im luftsstrom,   Forsch".   Geb. Ingenieurwes 4, 1933, 215-224.

3- T. Igarashi ,"Heat transfer from a square prism to an air stream",

Int. J . Heat Mass Transfer 28, 1985, 175-181.

4- T. Igarashi, "Local heat transfer from a square prism to an air stream", Int .J. Heat Mass Transfer 29, 1986, 777-784.

5- T. Igarashi, Fluid flow and heat transfer around rectangular cylinders (the case of a width/height ratio of 0.33~1.5), Int.J.Heat Mass Transfer 30, 1987, 893-901.

6- A. Valencia and C.orellana, Simulation of turbulent flow and heat transfer around rectangular bars, 26, 1999, 869-878.

7- A. Valencia, Turbulent flow and heat transfer in a channel with a square bar detached from the wall, Numer. Heat Transfer Part A 37, 2000, 289–306.

8- A. Valencia, Heat transfer enhancement in a channel with a built-in square cylinder.Interrnational Communications in Heat and Mass Transfer, 22 no1, 1995, 47-58.

9- D. A. Lyn, S. Einav, W. Rodi and J. H. Park, A Laser-Doppler Velocimetry Study of Ensemble-Averaged Characteristics of the Turbulent Near Wake of a Square Cylinder, Journal of Fluid Mechanics, 304, 1995, 285-319.

10- G. R. Ahmed& M. M. Yovanovich, Experimental Study of Forced Convection from Isothermal Circular and Square Cylinders and Toroids. Journal of Heat Transfer, 119, 1997, 70-79.

11- E. M. Sparrow, J. P. Abraham, J.C.K. Tong, Archival correlations for average heat transfer coefficients for non-circular and circular cylinders and for spheres in cross-flow.

International Journal of Heat and Mass Transfer 47, 2004, 5285–5296.

12- R. J. Goldstein, S. Y. Yoo, and M. K Chung, "Convective Mass Transfer from a Square Cylinder and Its Base Plate," Int. J. Heat Mass Transfer, 33, 1990, 9-18.

13- S.Y. Yoo, J.H. Park, C.H. Chung, M.K. Chung, An Experimental Study on Heat/Mass Transfer From a Rectangular Cylinder, Journal of Heat Transfer, 125,2003, 1163-1169.

14- A.K. Dhiman, R.P. Chhabra, V. Eswaran, Flow and heat transfer across a confined square cylinder in the steady flow regime: Effect of Peclet number, International Journal of Heat and Mass Transfer 48, 2005, 4598–4614.

15- M.A. Moussaoui, M. Jami, A. Mezrhab, H. Naji, MRT-Lattice Boltzmann simulation of forced convection in a plane channel with an inclined square cylinder, International Journal of Thermal Sciences 49, 2010, 131–142.

16- P. Koteswara Rao, C. Sasmal, A.K. Sahu, R.P. Chhabra, V. Eswaran, Effect of power-law fluid behavior on momentum and heat transfer characteristics of an inclined square cylinder in steady flow regime, International Journal of Heat and Mass Transfer 54, 2011, 2854-2867.

17- Sundus Hussein Abd, Experimental Study on the Impact of External Geometrical Shape on Free and Forced Convection Time Dependent Average Heat Transfer Coefficient during Cooling Process, Al-Khwarizmi Engineering Journal, Vol. 8, No.3, 2012, 74 - 89.
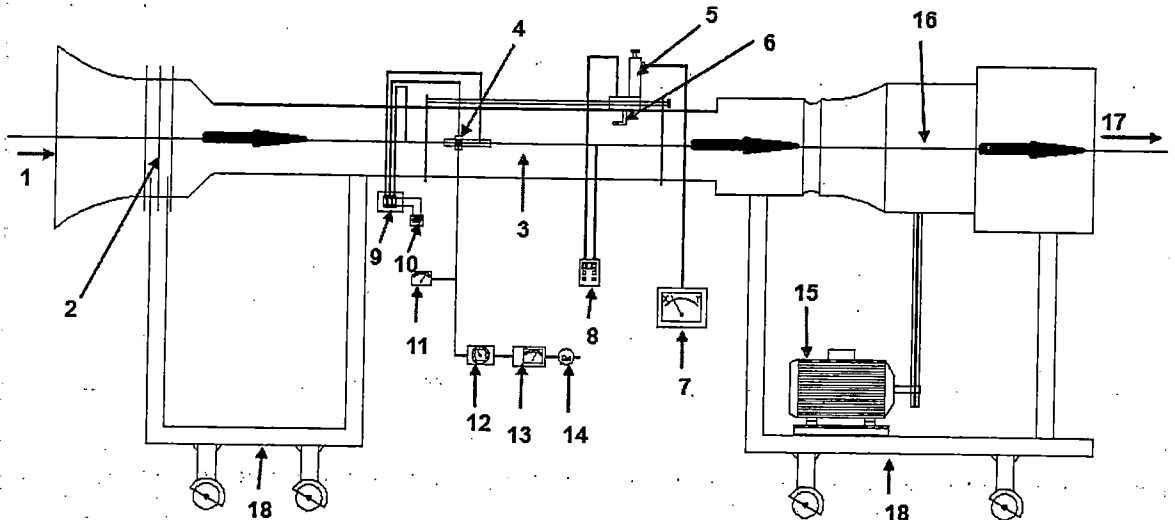
1-inlet
2- filters, honeycombs, damping screens
3-test section
4-bar
5- The traversing mechanism
6-Pitot tube

7-positioner
8-digital manometer
9-mult-point switch
10-digital control temperature
11-avometer
12-variac

13-stabilizer
14-electrical source
15-electrical motor
16-fan
17-outlet
18-base

Fig. 1 Experimental Set-up
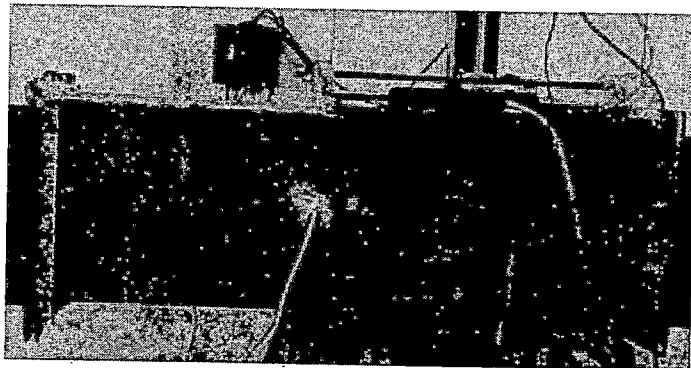
Fig. 2 photograph of test section
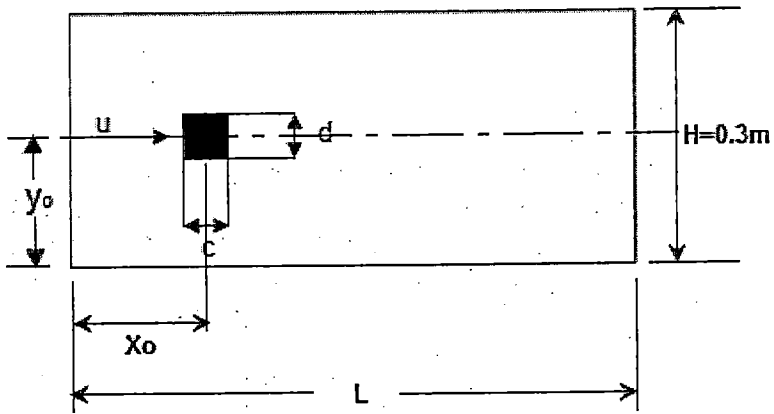
Fig. 3 Flow geometry
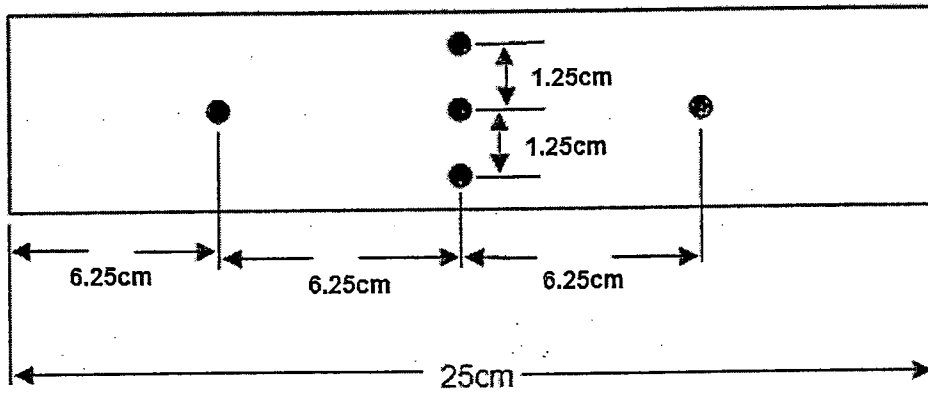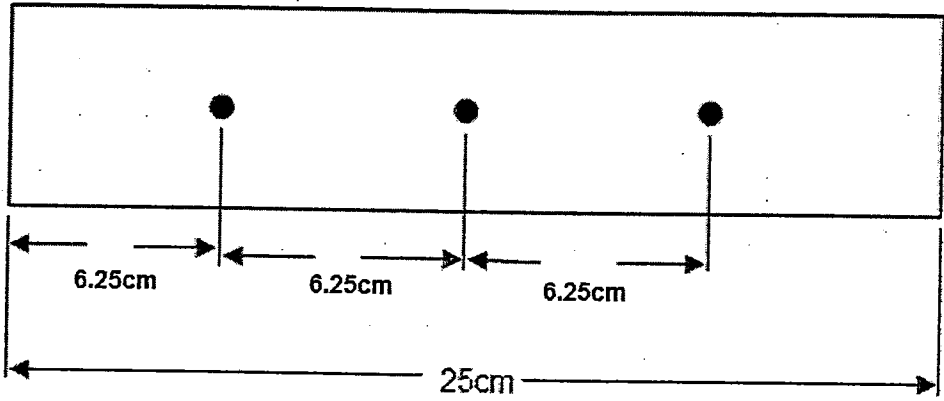

Fig.4 Position of thermocouples on upper face of the bar

Fig.5 Position of thermocouples on front, rear, lower faces of the bar
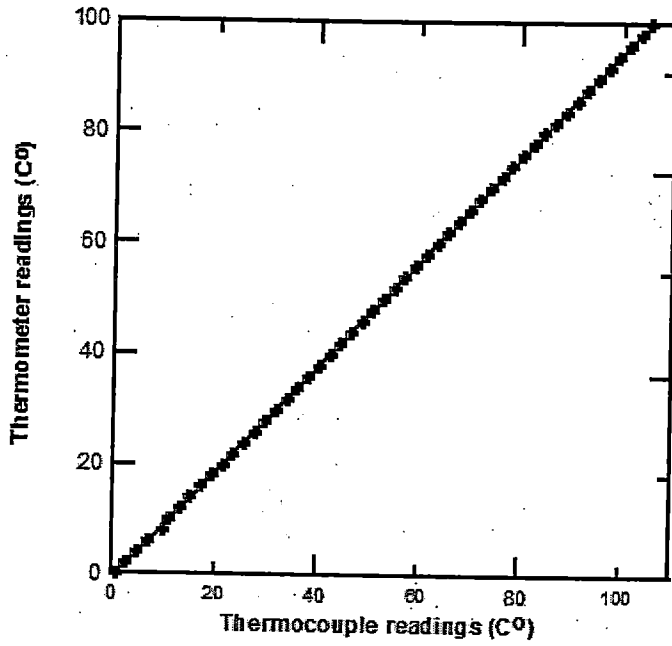
Fig. 6 Thermocouples calibration

$$\frac{\partial u}{\partial x} = 0$$

$$v = 0$$

$$\frac{\partial k}{\partial x} = 0$$

$$\frac{\partial \varepsilon}{\partial x} = 0$$
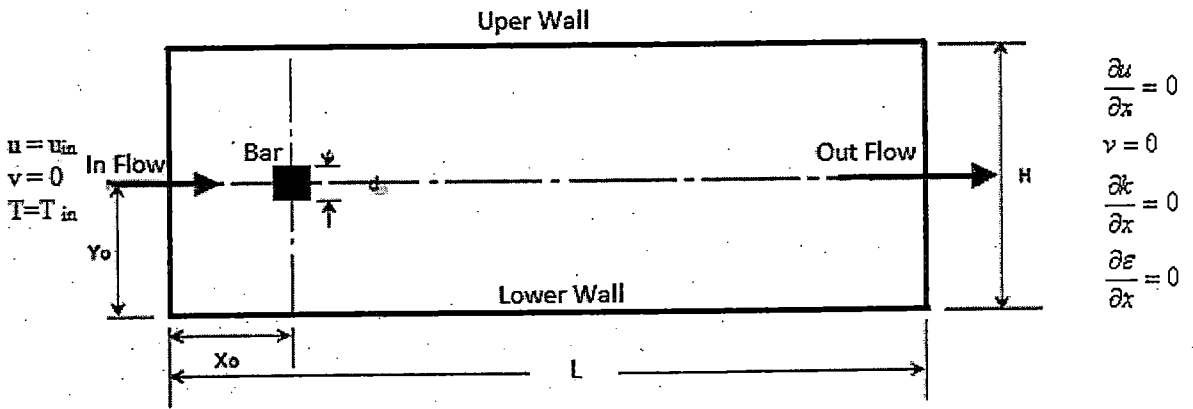
Fig. 7 Solution domain
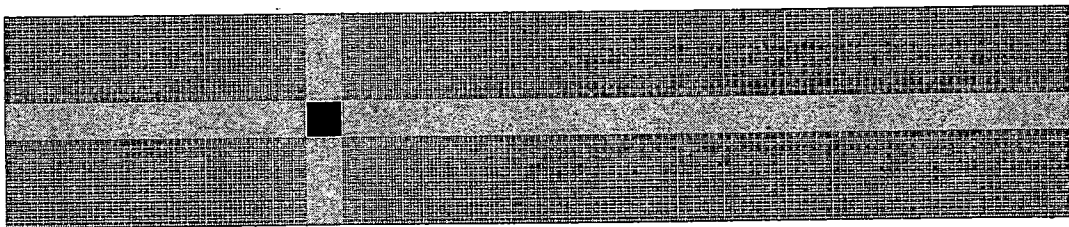
Fig. 8 Computational grid
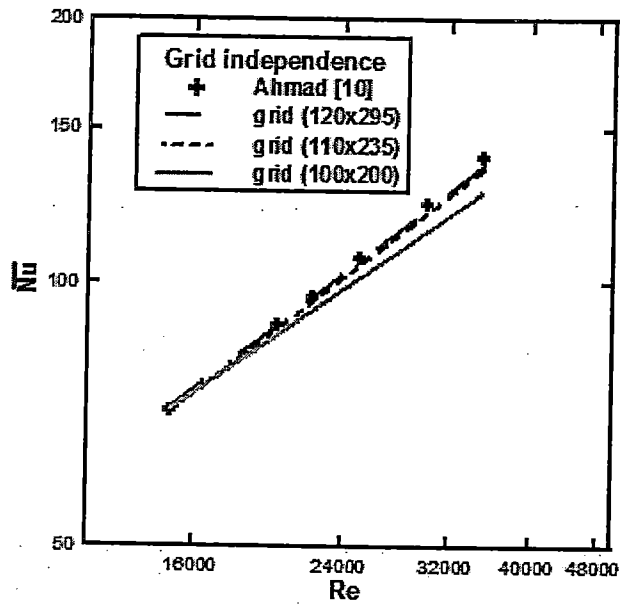
Fig. 9 Grid independence
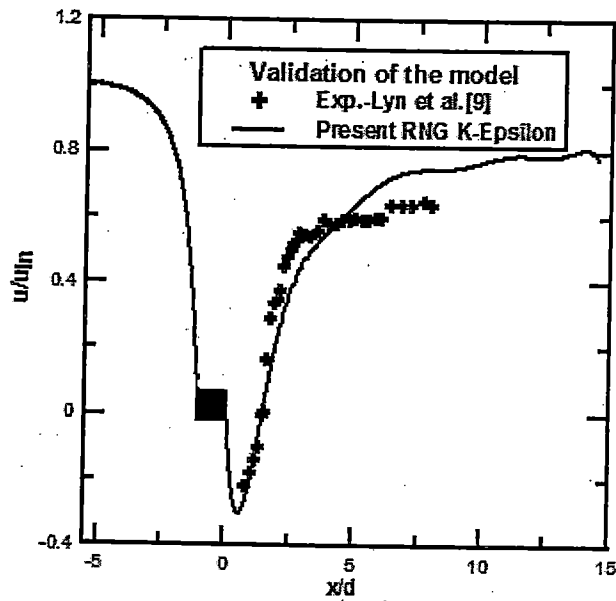
Fig. 10 Numerical x-velocity in centerline of test section compared with the experimental work of Lyn et al .[9]
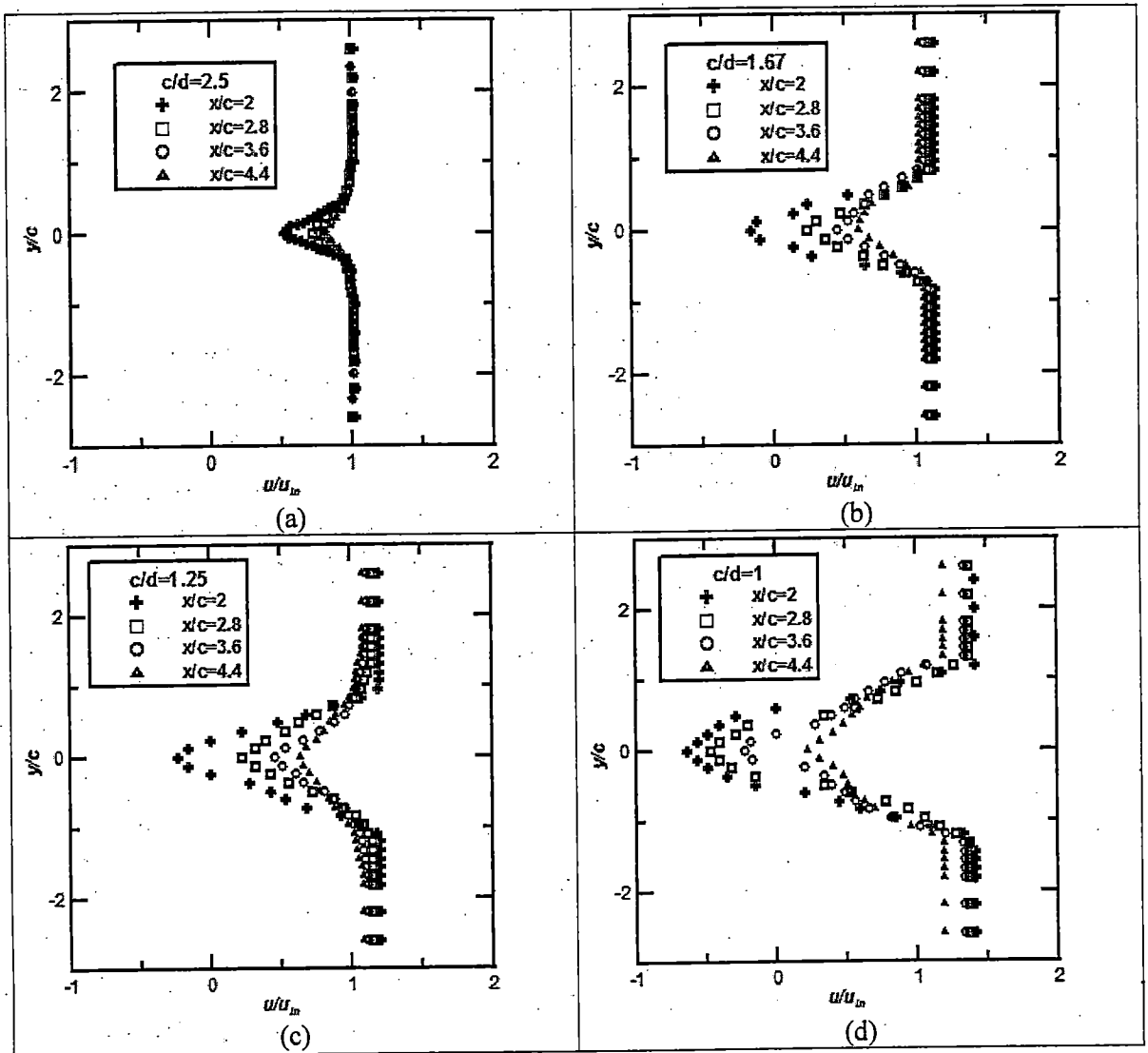
Fig. 11 Experimental velocity distribution behind the bar for Re=2.2*10^4
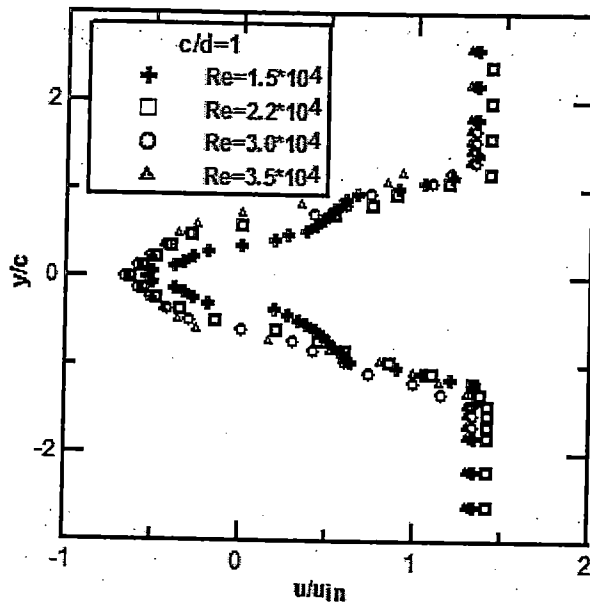
Fig.12 Experimental velocity distribution behind the bar for c/d=1& x/c=2
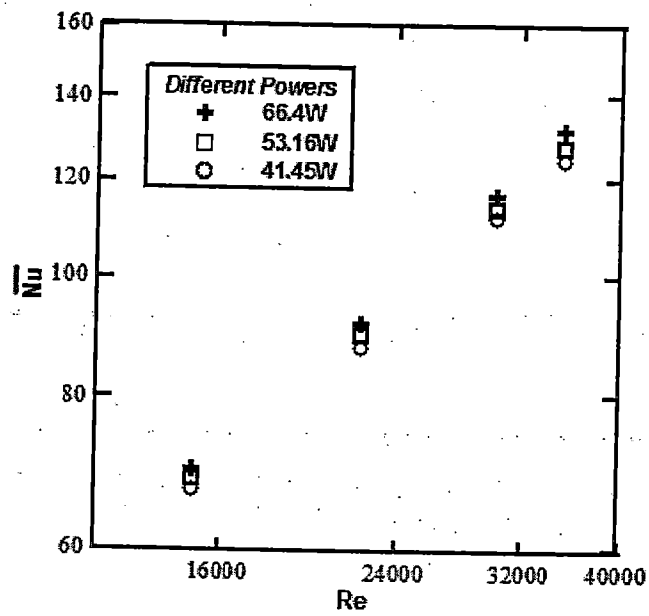
Fig. 13 Average Nusselt numbers with varying power for c/d=1
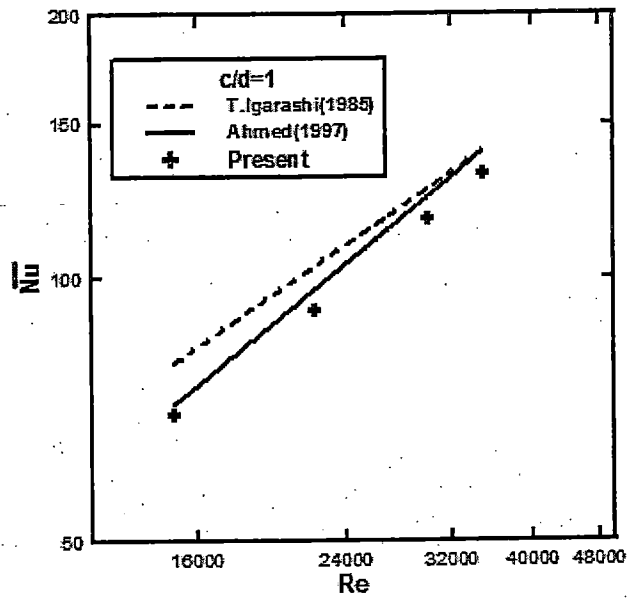
Fig. 14 Comparison between previous study works for c/d=1
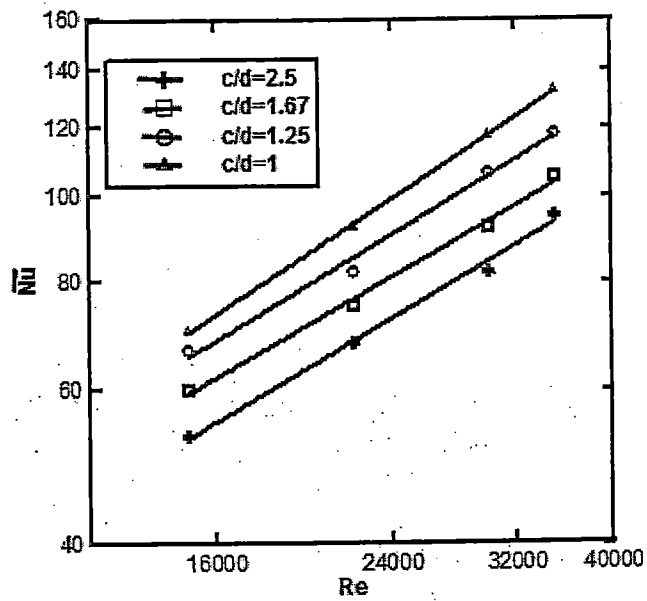
Fig. 15 Experimental Average Nusselt number on the bars
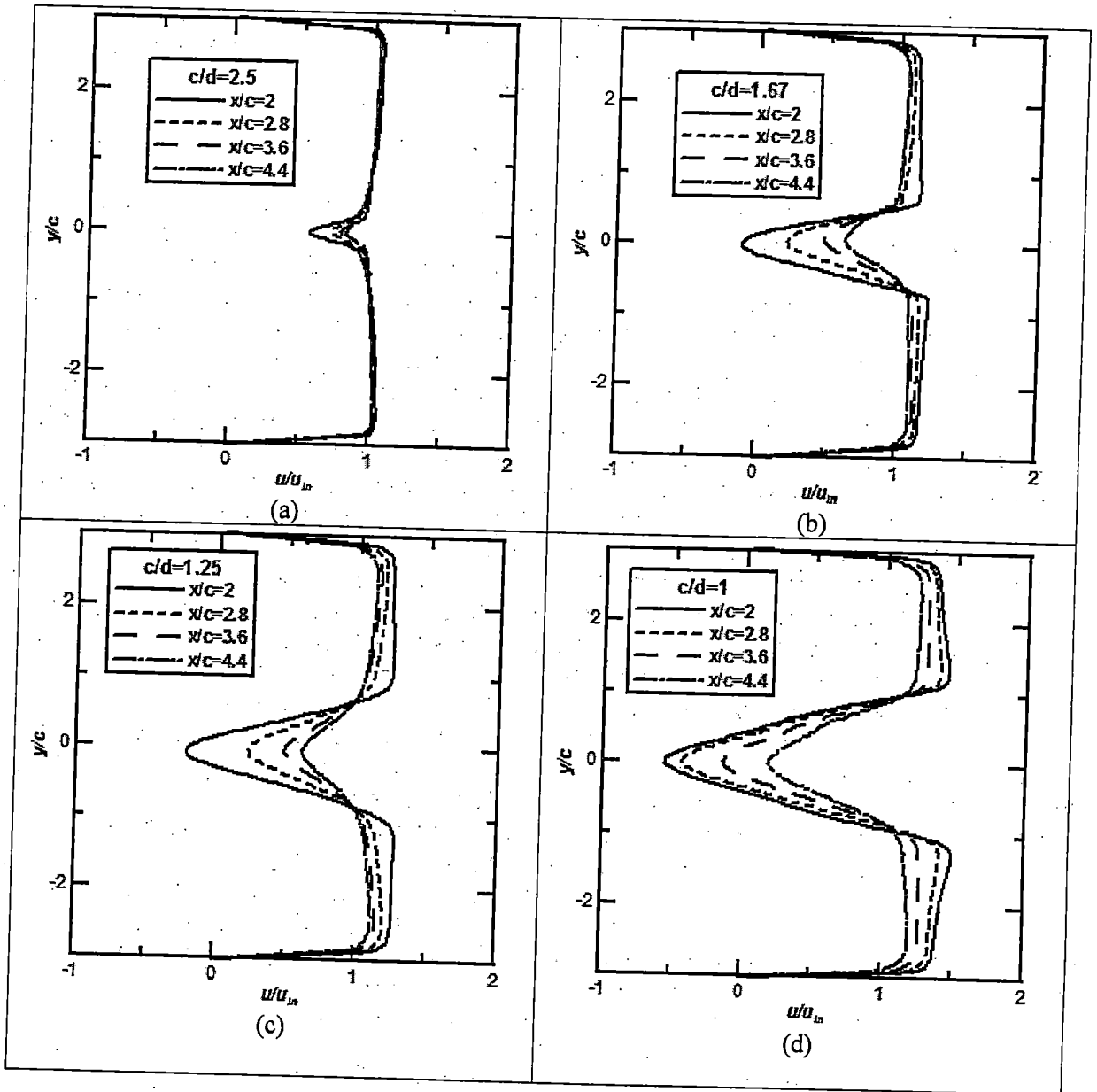
Fig.16 Numerical velocity distribution behind the bars at Re=2.2*10 ^{4}
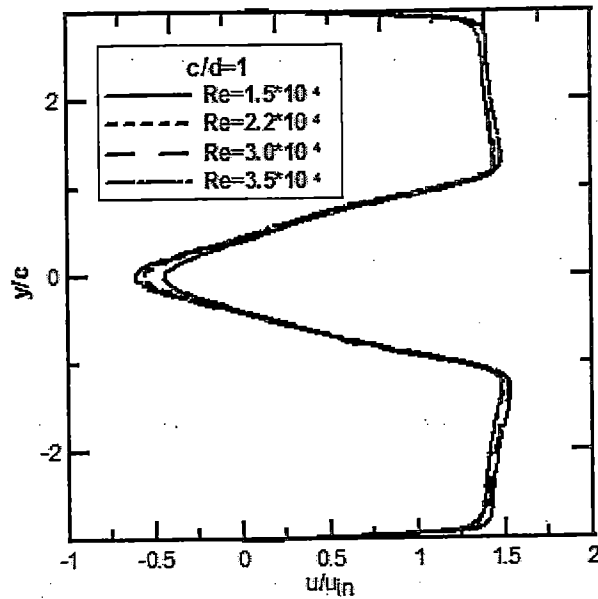
Fig.17 Numerical velocity distribution behind the bar for c/d=1& x/c=2
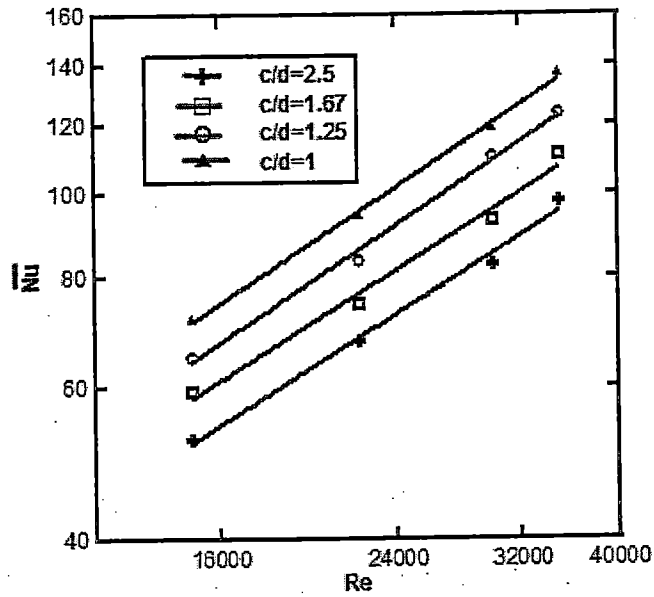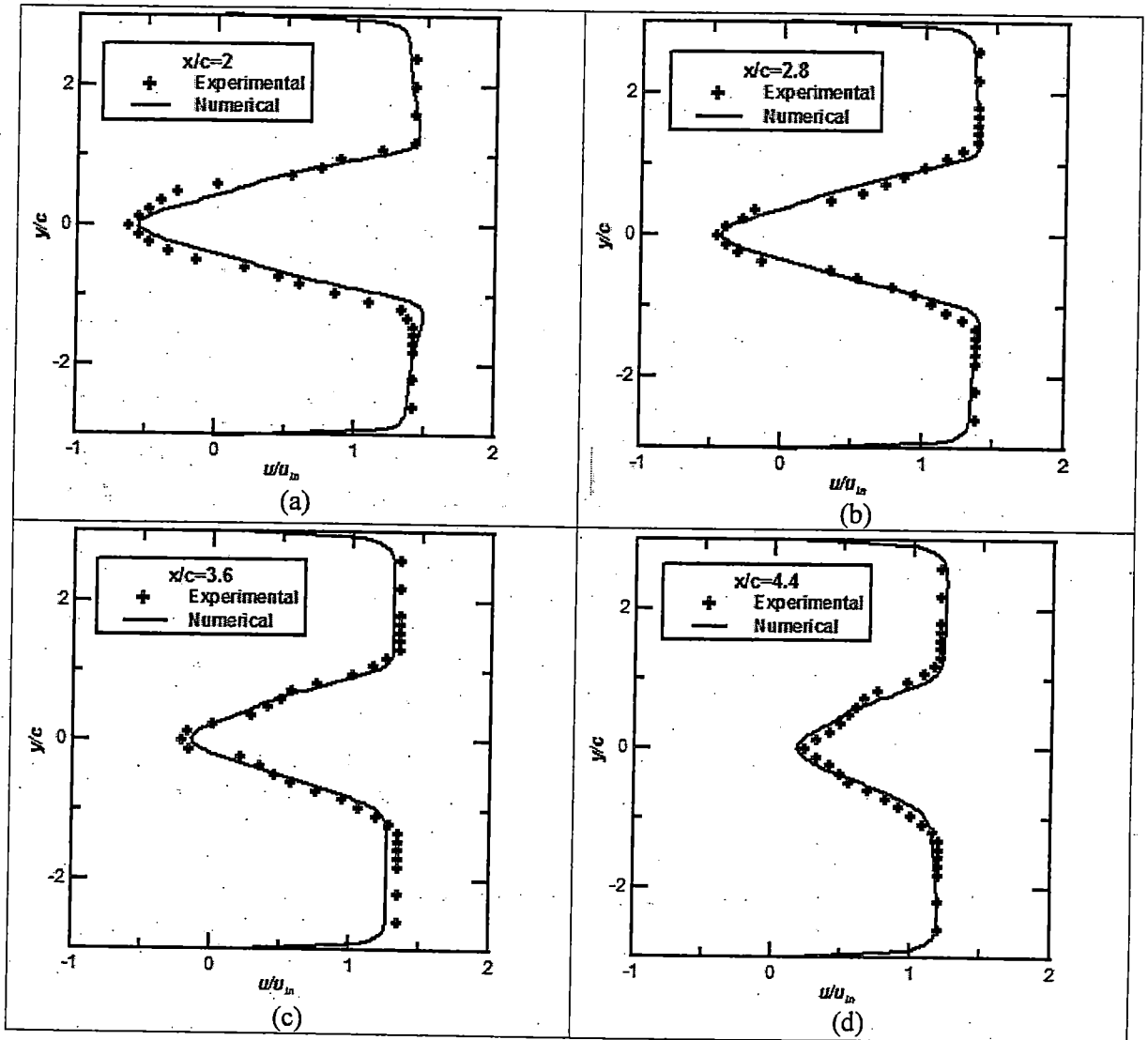

Fig.18 Numerical Average Nusselt number on the bars

Fig.19 Comparison between experimental and numerical results of velocity distribution behind the bar at Re=2.2*10.^{4}, c/d=1.
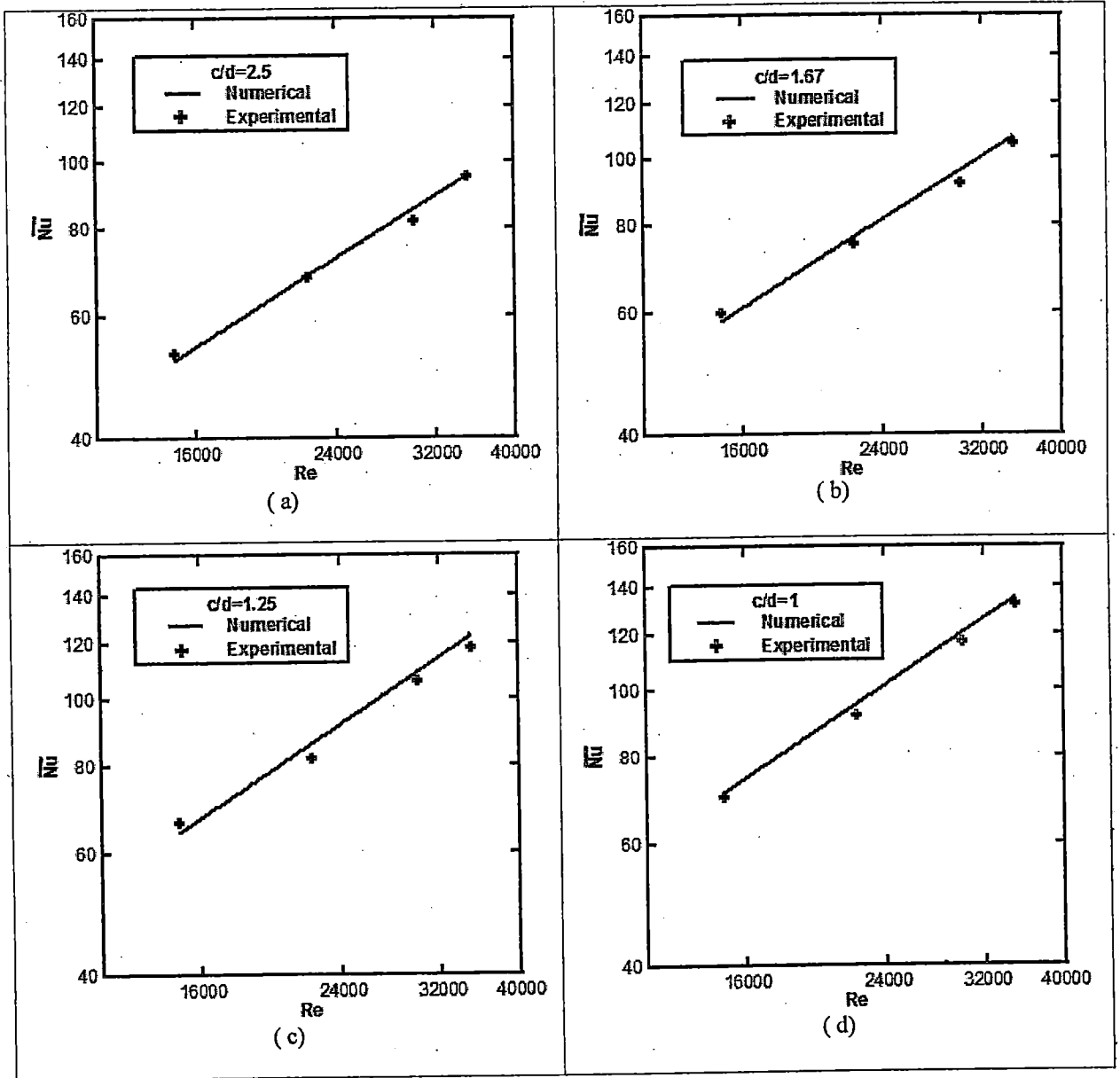
Fig. 20 Comparison between present experimental and numerical results of average Nusselt number for rectangular cross-section bars with versus Reynolds number